

Stepwise global error control in Euler's method using the DP853 triple and the Taylor remainder term

J. S. C. Prentice
 Senior Research Officer
 Mathsophical Ltd.
 Johannesburg, South Africa

March 20, 2023

Abstract

We report on a novel algorithm for controlling global error in a step-by-step (stepwise) sense, in the numerical solution of a scalar, autonomous, nonstiff or weakly stiff problem. The algorithm exploits the remainder term of a Taylor expansion of the solution. It requires the use of the DP853 triple to solve an auxiliary problem which, in turn, enables the remainder term to be determined. A *quenching* process then allows the solution generated by Euler's method to be controlled. We have achieved tolerances on the relative global error as strict as 10^{-10} .

2010 MSC: 65L05, 65L06, 65L70

Key words and phrases: Ordinary differential equations, Local error, Global error, Runge-Kutta, Error control

1 Introduction

We seek to solve numerically the real-valued scalar autonomous problem

$$\begin{aligned} y'(x) &= f(y) \\ y(x_0) &= y_0 \\ x &\in [x_0, x_N], \end{aligned} \tag{1}$$

using an algorithm based on Runge-Kutta methods, with *stepwise* (step-by-step) global error control. Work has been done on stepwise estimation and suppression of the global error in these types of problems, and we will discuss this in a later section. There, we will also refer to our own earlier work in this regard. In this brief introduction, it suffices to state that we intend to describe a novel approach to controlling the global error in Euler's method applied to (1), in a stepwise sense, by exploiting the remainder term of a low-order Taylor expansion. Our algorithm will make use of the DP853 embedded triple [9]. Remarkably enough, we have been able to achieve relative global error tolerances as strict as 10^{-10} .

2 Relevant Concepts

2.1 The Taylor-Lagrange function

Let $y(x)$ be a real-valued univariate function, and assume that $y(x)$ is as differentiable as is required in this paper. Taylor's theorem [34] provides the following result:

$$y(x) = y(x_0) + y'(\xi_x, \mu_x)(x - x_0) = y_0 + f(\mu_x)(x - x_0), \quad (2)$$

where $\mu_x = y(\xi_x)$ and $x_0 < \xi_x < x$. The second term on the RHS is the *remainder term*, presented here in *Lagrange* form [1],[3]. By differentiating (2) with respect to x , we find

$$\begin{aligned} y'(x) &= f(\mu_x) + (x - x_0) \frac{\partial f(\mu_x)}{\partial \mu_x} \frac{d\mu_x}{dx} \\ &= f(\mu_x) + f_y(\mu_x)(x - x_0) \frac{d\mu_x}{dx}. \end{aligned} \quad (3)$$

Now, the LHS of this expression exists (see (1)), and so we will assume that the RHS also exists. Hence, we assume that $\frac{d\mu_x}{dx}$ exists. This suggests that μ_x is a function of x , and we will sometimes write $\mu(x)$ or simply μ in place of μ_x . We will refer to μ_x as the *Taylor-Lagrange function*, or simply *Lagrange function*, for this particular situation. In (2) and (3), we have used the notation

$$\begin{aligned} y'(\xi_x, \mu_x) &\equiv y'(\mu(x)) = f(\mu(x)) \equiv f(\mu_x) \\ y''(\xi_x, \mu_x) &\equiv \frac{dy'(\mu(x))}{d\mu(x)} = \frac{dy'(y)}{dy} \bigg|_{y=\mu_x} = \frac{df}{dy} \bigg|_{y=\mu_x} \equiv f_y(\mu_x). \end{aligned}$$

Rearranging (3) and using (1) and (2) gives

$$\begin{aligned}
\frac{d\mu}{dx} &= \frac{f(y) - f(\mu)}{f_y(\mu)(x - x_0)} \\
&= \frac{f(y_0 + f(\mu)(x - x_0)) - f(\mu)}{f_y(\mu)(x - x_0)} \\
&\equiv g(x, \mu).
\end{aligned} \tag{4}$$

This is an initial-value problem that can, in principle, be solved to yield the Lagrange function $\mu(x)$ for a suitable initial value. Once $\mu(x)$ is known, the remainder term $f(\mu)(x - x_0)$ is easily computed. Then, adding the remainder term to $y(x_0)$ yields, from (2), an approximation to $y(x)$. For interest's sake, we refer the reader to our recent work in this regard [19].

2.2 Runge-Kutta Methods

The topic of Runge-Kutta (RK) methods is very broad, indeed. We will assume the reader has suitable familiarity with these methods, and list Butcher [4] as a good general reference. Here, we will simply establish notation and terminology relevant to this paper.

To solve $\mu' = g(x, \mu)$ numerically, we partition $[x_0, x_N]$ using the nodes $x_0 < x_1 < \dots < x_N$ and we use the RK method

$$\mu_{i+1} = \mu_i + h_{i+1} \Phi(x_i, \mu_i).$$

Here, μ_i and μ_{i+1} are the approximate numerical solutions at x_i and x_{i+1} , respectively, $h_{i+1} \equiv x_{i+1} - x_i$ is the *stepsize*, and $\Phi(x, \mu)$ is known as the *increment function*. The increment function defines the RK method. We will make use of several RK methods in this work - denoted RK1, RK4, RK7 and DP853 - and we will describe them when appropriate. Also, the consistency property of RK methods means that

$$\begin{aligned}
\lim_{h_{i+1} \rightarrow 0} \Phi(x_i, \mu_i) &= g(x_i, \mu_i) \\
\lim_{h_{i+1} \rightarrow 0} \Phi_\mu(x_i, \mu_i) &= g_\mu(x_i, \mu_i) \\
\lim_{h_{i+1} \rightarrow 0} \Phi_{\mu\mu}(x_i, \mu_i) &= g_{\mu\mu}(x_i, \mu_i),
\end{aligned} \tag{5}$$

where the subscript μ denotes partial differentiation with respect to μ .

2.2.1 The DP853 embedded triple

The DP853 embedded triple [9] comprises three RK methods (of orders 3, 5 and 8) that use differing combinations of the same internal stages to generate

their output. There are 12 stages in DP853, each of which has the general form

$$k_q = h_{i+1}g(x_i + c_q h_{i+1}, \mu_i^V + a_{q,1}k_1 + a_{q,2}k_2 + \dots + a_{q,q-1}k_{q-1})$$

for each $q \in [1, 2, 3, \dots, 12]$. The methods are explicit, so that each stage is dependent on the previous stages, and they must be computed sequentially. We use the superscripts L , H and V to denote the third-, fifth- and eighth-order solutions, respectively. Hence, the outputs of DP853 are given by

$$\begin{aligned} \mu_{i+1}^L &= \mu_i^L + \sum_{q=1}^{12} b_q^L k_q \equiv \mu_i^L + h_{i+1} \Phi^L(x_i, \mu_i^L) \\ \mu_{i+1}^H &= \mu_i^H + \sum_{q=1}^{12} b_q^H k_q \equiv \mu_i^H + h_{i+1} \Phi^H(x_i, \mu_i^H) \\ \mu_{i+1}^V &= \mu_i^V + \sum_{q=1}^{12} b_q^V k_q \equiv \mu_i^V + h_{i+1} \Phi^V(x_i, \mu_i^V) \end{aligned} \quad (6)$$

wherein we have implicitly defined coefficients b_q^{\dots} and appropriate increment functions. It transpires that DP853 has $b_q^{H,V} = 0$ for $q \in [2, 3, 4, 5]$ and $b_q^L = 0$ for $q \in [2, 3, 4, 5, 6, 7, 8, 10, 11]$.

We modify (6) slightly: we use μ_i^H as input for μ_{i+1}^L , i.e.

$$\mu_{i+1}^L = \mu_i^H + \sum_{q=1}^{12} b_q^L k_q. \quad (7)$$

We discuss the value of this approach in the next subsection.

2.3 Local and Global Error

The RK *local error* at x_{i+1} is

$$\delta_{i+1} \equiv \mu(x_{i+1}) - (\mu(x_i) + h_{i+1} \Phi(x_i, \mu(x_i)))$$

and the RK global error at x_{i+1} is

$$\Delta_{i+1} \equiv \mu(x_{i+1}) - \mu_{i+1} = \mu(x_{i+1}) - (\mu_i + h_{i+1} \Phi(x_i, \mu_i)),$$

where $\mu(x_i)$ and $\mu(x_{i+1})$ are the exact solutions at x_i and x_{i+1} , respectively. The difference between the two concepts is subtle: the local error definition requires that $\mu(x_i)$ is known.

An RK method of *order* p , written RK_p , has

$$\delta_{i+1} \propto h_{i+1}^{p+1} + \dots = L_{i+1} h_{i+1}^{p+1} + \dots \quad (8)$$

$$\Delta_{i+1} \propto h^p + \dots = G_{i+1} h^p + \dots \quad (9)$$

In the latter expression, the symbol h represents the mean stepsize over the subinterval $[x_0, x_{i+1}]$. The ellipses represent higher-order terms.

The local and global errors are related. We have shown [20][21] that

$$\Delta_{i+1} = \delta_{i+1} + \Delta_i + h_{i+1} \Phi_\mu(x_i, \mu_i) \Delta_i + \dots \quad (10)$$

where Δ_i is the global error in the input μ_i . Hence, ignoring higher order terms, (7) yields

$$\Delta_{i+1}^L = \delta_{i+1}^L + (1 + h_{i+1} \Phi_\mu(x_i, \mu_i^H)) \Delta_i^H.$$

Compare this with

$$\Delta_{i+1}^L = \delta_{i+1}^L + (1 + h_{i+1} \Phi_\mu(x_i, \mu_i^L)) \Delta_i^L$$

which follows from (6). The second term on the RHS is the contribution to Δ_{i+1}^L due to the global error of the input μ_i^H or μ_i^L . Since we expect $|\Delta_i^H| \ll |\Delta_i^L|$, we see that (7) reduces the magnitude of Δ_{i+1}^L compared with what it would otherwise have been.

2.4 Error Control

2.4.1 Local error

It is possible to adjust the stepsize so as to control the local error. If $\varepsilon_\delta > 0$ denotes a user-defined tolerance on the local error, then

$$|\delta_{i+1}| = |L_{i+1} h_i^{p+1}| \leq \varepsilon_\delta \Rightarrow h_{i+1} \leq \left(\frac{\varepsilon_\delta}{|L_{i+1}|} \right)^{\frac{1}{p+1}}$$

provides an estimate of the stepsize necessary to bound $|\delta_{i+1}|$. In this expression we have ignored higher-order terms present in the expansion of δ_{i+1} (see (8)). To cater for this omission, it is common practice to use a *safety factor* $0 < \eta < 1$, so that we have

$$h_{i+1} = \eta \left(\frac{\varepsilon_\delta}{|L_{i+1}|} \right)^{\frac{1}{p+1}}$$

as the desired value of h_{i+1} . We will use $\eta = 0.85$ throughout this study. Furthermore, it is possible to control the *local error density* ρ_{i+1} , or *local error per unit step* as it is often known,

$$\rho_{i+1} \equiv \frac{|\delta_{i+1}|}{h_i} = |L_{i+1}h_{i+1}^p| \leq \varepsilon_\rho \Rightarrow h_{i+1} = \eta \left(\frac{\varepsilon_\rho}{|L_{i+1}|} \right)^{\frac{1}{p}}, \quad (11)$$

where $\varepsilon_\rho = \varepsilon_\delta/h_{i+1}$.

There are two virtues in controlling the error density. Firstly, the exponent is larger $\left(1 > \frac{1}{p} > \frac{1}{p+1}\right)$ and, anticipating that $\frac{\varepsilon_\rho}{|L_{i+1}|} \ll 1$, we will find that h_{i+1} will be smaller, meaning that $|\delta_{i+1}| \leq \varepsilon_\delta$ is satisfied, as well.

Secondly, if h_{i+1} is suitably small we find, from (10), the recursion

$$\Delta_{i+1} = \delta_{i+1} + \Delta_i \Rightarrow \Delta_{i+1} \leq |\delta_{i+1}| + \Delta_i. \quad (12)$$

With $\Delta_0 = 0$ (because the initial value is known exactly) and assuming $|\delta_{i+1}| \leq \varepsilon_\rho h_{i+1}$, we find

$$\Delta_N \leq \varepsilon_\rho \sum_{i=0}^{N-1} h_{i+1} = \varepsilon_\rho (x_N - x_0).$$

The recursion (12) is monotonically increasing, so that $\varepsilon_\rho (x_N - x_0)$ is a rough bound on the global error that can be made *a priori*. Hence, for a desired value of Δ_N , we could estimate the necessary local tolerance ε_ρ via

$$\varepsilon_\rho \leq \frac{\Delta_N}{x_N - x_0}. \quad (13)$$

We prefer to control *relative* error, as in

$$\frac{\rho_{i+1}}{|\mu_{i+1}|} \equiv \frac{|\delta_{i+1}|}{|\mu_{i+1}| h_{i+1}} \leq \varepsilon_\rho \Rightarrow h_{i+1} = \eta \left(\frac{\varepsilon_\rho |\mu_{i+1}|}{|L_i|} \right)^{\frac{1}{p}}, \quad (14)$$

when $|\mu_{i+1}| > 1$, and *absolute* error, as in (11), when $|\mu_{i+1}| \leq 1$. The difference between the two cases is in the numerator on the RHS of (14).

For relative error control, we have $\rho_{i+1} \leq \varepsilon_\rho |\mu_{i+1}|$, and for absolute error control we have $\rho_{i+1} \leq \varepsilon_\rho$. These two cases can be conveniently expressed as

$$\rho_{i+1} \leq \varepsilon_\rho \max(1, |\mu_{i+1}|).$$

The RHS is a *hinge* function (of $|\mu_{i+1}|$), and is somewhat different to the often-used linear expression

$$\rho_{i+1} \leq \varepsilon_\rho (1 + |\mu_{i+1}|).$$

We see that the linear expression gives $\rho_{i+1} \leq \varepsilon_\rho$ only when $|\mu_{i+1}| = 0$. For all other values of $|\mu_{i+1}|$, the bound imposed on ρ_{i+1} is larger than ε_ρ or, since $\rho_{i+1}/|\mu_{i+1}| \leq \varepsilon_\rho (1/|\mu_{i+1}| + 1)$, the bound imposed on $\rho_{i+1}/|\mu_{i+1}|$ is larger than ε_ρ . Hence, we prefer to use the hinge function, since it respects the user-defined bound ε_ρ .

2.4.2 Global error

Global error control is a more difficult task, particularly in a stepwise sense. The easiest implementable form of global error control requires an estimation of the error after the integration has been done, and then solving the problem again using a new, smaller stepsize. This is known as *reintegration*, and is an *a posteriori* form of control. Much work has been done regarding global error estimation (see, for example, [2][5][6][7][8][10][11][12][16][17][32][33][36]). However, there are cases to be made for controlling the global error as the integration proceeds [23][26][27][28][29][30][31]. In this regard, much less work has been done. The quasi-consistent peer methods (see [13][14][15][35][36] and many references therein) have shown very good performance, particularly when dealing with strongly stiff systems, but these methods are not quite *stepwise* control methods. They typically require a "reboot" of the method when a certain tolerance has been breached, which results in the method having to backtrack several, perhaps many, nodes, resulting in what is effectively a partial reintegration. In this paper, and in our other work [22][24][25][26][27], we insist on a backtrack of no more than a single node, when required, using a process we refer to as *quenching*.

3 The Algorithm

We intend to construct an algorithm that will allow for local control of the global error in a RK1 method, by determining the remainder term in (2). This is a more subtle approach than the direct extrapolation technique we have previously used [22][24][25]. We believe the best way to describe our algorithm is in a step-by-step manner that follows the sequential implementation of the algorithm itself.

1. Using $f(y)$ and (1), we construct $g(x, \mu)$.
2. We choose a point x_μ very close to x_0 , and use a high-order RK method - such as RK4 or even RK7 - to find a solution y_μ of (1) at x_μ . We assume y_μ to be sufficiently accurate so as to be regarded as practically

exact. From (2), we then have

$$y_\mu - y_0 - f(\mu)(x_\mu - x_0) = 0,$$

which can be solved using a nonlinear solver to find μ (see the Appendix; there is an important subtlety to consider). We label this value μ_1 and we relabel x_μ as x_1 . Moreover, we observe that (2) is trivially satisfied when $x = x_0$, so that μ is arbitrary at x_0 . There is no harm, then, in setting $\mu_0 = 0$. This labelling is merely a logistical convenience, and it provides the ordered pairs $\{(x_0, \mu_0), (x_1, \mu_1)\}$ as the first two values in our numerical solution for μ . **NB:** We also relabel y_μ as y_1 .

3. We now use a pair of RK methods to determine μ at $x_2 = x_1 + h_2$, with (x_1, μ_1) as input. The stepsize h_2 is user-defined (more on this point later). These RK methods are the third- and fifth-order components of the DP853 embedded triple. We need two values of μ at x_2 , obtained with methods of differing order, to be able to implement local error control. We will denote these two solutions μ_2^L and μ_2^H . Using DP853 sets the order parameter $p = 3$ in the steps that follow. However, other users may choose to use RK methods of different orders, so we will persist in using the symbol p for the sake of generality.
4. The next step is to implement **local error control** (LEC) in μ at x_2 . We assume that μ_2^H is sufficiently accurate, relative to μ_2^L , such that

$$\mu_2^H - \mu_2^L = L_2 h_2^{p+1} \Rightarrow L_2 = \frac{\mu_2^H - \mu_2^L}{h_2^{p+1}}$$

is feasible. We now set $\mu_2 = \mu_2^H$ and apply the process

$$\begin{aligned} |\mu_2| > 1 \text{ and } |L_2 h_2^p| > \varepsilon_\rho |\mu_2| \Rightarrow h_2 &= \eta \left(\frac{\varepsilon_\rho |\mu_2|}{|L_2|} \right)^{\frac{1}{p}} \\ |\mu_2| \leq 1 \text{ and } |L_2 h_2^p| > \varepsilon_\rho \Rightarrow h_2 &= \eta \left(\frac{\varepsilon_\rho}{|L_2|} \right)^{\frac{1}{p}} \end{aligned}$$

to compute a new stepsize, if necessary. We refer to this error control as *primary* LEC.

There is a potentially valuable refinement that we can implement at this stage. Recall that we intend to determine the remainder term $f(\mu)(x - x_0)$. If we assume $\mu_2 \approx \mu(x_2) - L_2 h_2^{p+1}$ then we have

$$\begin{aligned} f(\mu_2)(x_2 - x_0) &= f(\mu(x_2) - L_2 h_2^{p+1})(x_2 - x_0) \\ &= f(\mu(x_2))(x_2 - x_0) - L_2 h_2^{p+1} f_y(\mu(x_2))(x_2 - x_0). \end{aligned}$$

The term $L_2 h_2^{p+1} f_y(\mu(x_2))(x_2 - x_0) \approx L_2 h_2^{p+1} f_y(\mu_2)(x_2 - x_0)$ can be thought of as a local error in $y_0 + f(\mu_2)(x_2 - x_0)$. We can apply the same reasoning as above to compute a new stepsize for a given tolerance on this particular local error, as in

$$\begin{aligned} \frac{|L_2 f_y(\mu_2)(x - x_0)| h_2^{p+1}}{h_2 \max(1, |y_0 + f(\mu_2)(x_2 - x_0)|)} &\leq \varepsilon_\rho \\ \Rightarrow h_2 &= \eta \left(\frac{\varepsilon_\rho \max(1, |y_0 + f(\mu_2)(x_2 - x_0)|)}{|L_2 f_y(\mu_2)(x_2 - x_0)|} \right)^{\frac{1}{p}}. \end{aligned} \quad (15)$$

Note the hinge function in the numerator. The division by h_2 corresponds to *error per unit step* control. If this value of h_2 is smaller than the value obtained from the earlier process, then it is chosen as the new stepsize. We refer to this error control as *secondary* LEC. Now, given that we propagate μ_1^H in DP3 (see (7)) and that, for strict tolerances, stepsizes may generally be small, $L_2 h_2^{p+1}$ may be a good approximation to the global error Δ_2 . Consequently, (15) constitutes a form of global error control, or at least global error suppression, in $y_0 + f(\mu_2)(x_2 - x_0)$. This is because the quantity $\Delta_2 f_y(\mu(x_2))(x_2 - x_0)$ is the global error in $y_0 + f(\mu_2)(x_2 - x_0)$. The nett result is that secondary LEC will likely lead to small global errors in $y_0 + f(\mu_2)(x_2 - x_0)$, a favourable and useful outcome. Secondary LEC should be used with some caution, however. In general, the denominator contains the factor $(x_i - x_0)$ which could become large for large intervals. This might lead to excessively small values for h_i . Perhaps a lower limit on the stepsize should be considered to counteract this. Perhaps the secondary LEC stepsize should not be allowed to be smaller than one-tenth of the primary LEC stepsize, say. We did not need to use such a lower limit in our numerical calculations, but it is something that is worth considering.

Effectively, what we have done here is to attempt to control the relative local error per step in both μ_2 and $y_0 + f(\mu_2)(x_2 - x_0)$. We then compute a new value for μ_2 using the new stepsize (i.e. we repeat Step 3 using the new stepsize), and then use the new values for μ_2^L and μ_2^H so obtained to find a new value for L_2 . In the event that no stepsize adjustment is necessary, we simply proceed directly to step 5 (note: in the event of repeating Step 3, we do *not* then repeat Step 4, as well - we move directly to step 5).

5. The global error in μ_2 can now be estimated using

$$\Delta_2 = \mu_2^V - \mu_2^L$$

where μ_2^V is the eighth-order solution from DP853. We prefer to overestimate Δ_2 , so we do not use $\Delta_2 = \mu_2^V - \mu_2^H$, even though we have set $\mu_2 = \mu_2^H$. Of course, it is the relative global error

$$\Delta_2^{rel} \equiv \frac{\Delta_2}{\max(1, |\mu_2|)}$$

that actually interests us.

6. We use Euler's Method (RK1) to find y_2 , as in

$$y_2 = y_1 + h_2 f(y_1).$$

It is, of course, the global error in y_2 that we ultimately wish to control.

7. We find the remainder term

$$R_2 = f(\mu_2)(x_2 - x_0).$$

8. We estimate the relative global error in the remainder term ΔR_2 by

$$\begin{aligned} f(\mu_2)(x_2 - x_0) &= f(\mu(x_2) - \Delta_2)(x_2 - x_0) \\ &\approx f(\mu(x_2))(x_2 - x_0) - f_y(\mu_2)(x_2 - x_0)\Delta_2 \\ &\quad + \frac{f_{yy}(\mu_2)(x_2 - x_0)\Delta_2^2}{2} \\ \Rightarrow \Delta R_2 &= \frac{f_{yy}(\mu_2)(x_2 - x_0)\Delta_2^2 - 2f_y(\mu_2)(x_2 - x_0)\Delta_2}{2\max(1, |R_2|)}. \end{aligned}$$

9. We now have the Euler solution y_2 and the Taylor approximation

$$\begin{aligned} y_2^T &= y_0 + f(\mu_2)(x_2 - x_0) \\ &\approx \underbrace{[y_0 + f(\mu(x_2))(x_2 - x_0)]}_{y(x_2)} + \Delta R_2. \end{aligned}$$

The term in square brackets is the exact solution $y(x_2)$. Therefore, if ΔR_2 is suitably small,

$$\Delta y_2 \approx y_2^T - y_2,$$

where Δy_2 denotes the global error in y_2 . In fact, we measure the relative global error

$$\Delta y_2^{rel} \equiv \frac{\Delta y_2}{\max(1, |y_2^T|)} \approx \frac{y_2^T - y_2}{\max(1, |y_2^T|)}$$

and we test the inequality

$$|\Delta y_2^{rel}| > |\varepsilon_g - |\Delta y_2^T||, \quad (16)$$

where $\varepsilon_g > 0$ is a user-defined tolerance on the relative global error in the Euler solution, and

$$\Delta y_2^T \equiv \frac{f_{yy}(\mu_2)(x_2 - x_0)\Delta_2^2 - 2f_y(\mu_2)(x_2 - x_0)\Delta_2}{2 \max(1, |\Delta y_2^T|)}.$$

If (16) is true we **quench** the Euler solution y_2 by setting

$$y_2 = y_0 + f(\mu_2)(x_2 - x_0),$$

confident that

$$|\Delta y_2^{rel}| \leq \max(\varepsilon_g, |\Delta y_2^T|).$$

Of course, we prefer that $|\Delta y_2|$ be bounded by the imposed tolerance ε_g , and it is likely that it will be if **strict** local error control has been carried out earlier (small ε_ρ). But even if $|\Delta y_2^T| > \varepsilon_g$ so that $|\Delta y_2^T|$ is effectively the bound on $|\Delta y_2^{rel}|$, at least we know the value of $|\Delta y_2^T|$. In such a case, if $|\Delta y_2^T|$ is acceptably small, we would still be satisfied with the result.

NB: It is imperative to track the growth of $|\Delta y_2^T|$ and, if $|\Delta y_2^T|$ becomes too large, we backtrack to a node x_k where $|\Delta y_k^T|$ is acceptably small, and then repeat the process from Step 1. That is to say, we treat (x_k, y_k^T) as a new initial value (x_0, y_0) and "reboot" the algorithm from this new initial value. This reboot process is executed *only if it is deemed necessary*.

Obviously, if the test (16) is false, we do not quench the solution, and simply proceed to the next step. An argument can be made that one should always quench while $|\Delta y_2^T|$ is acceptably small. We have chosen not to do this in our numerical examples, in order to make explicit the effects of quenching and not quenching. Nevertheless, persistent quenching does have its merits.

10. We now have a solution y_2 that satisfies a tolerance on its global accuracy. Furthermore, this error control has been implemented in a stepwise (local) manner. We are ready to compute y_3 . We return to Step 3, **update the indices by one** and continue until we eventually reach the endpoint x_N .

4 Numerical Examples

We consider the following examples for the purpose of numerical experiments:

Table 1: Details of numerical examples

#	ODE	Interval	y_0	Solution
1	$y' = y$	$[0, 5]$	2	$y(x) = 2e^x$
2	$y' = y^2$	$[-10, -3]$	0.1	$y(x) = -\frac{1}{x}$
3	$y' = \frac{y}{4} \left(1 - \frac{y}{20}\right)$	$[0, 20]$	1	$y(x) = \frac{20}{1+19e^{-x/4}}$
4	$y' = \frac{1}{y}$	$[5, 25]$	1	$y(x) = \sqrt{2x - 9}$
5	$y' = \cos y$	$[a, b]$	-1	$x = \ln(\sec y + \tan y)$
6	$y' = -y$	$[0, 10]$	1	$y(x) = e^{-x}$

where, in #5,

$$\begin{aligned} a &= -1.2261911708835170708130609674719 \\ b &= 1.2261911708835170708130609674719. \end{aligned}$$

Some of these problems are weakly stiff, and the solution in #5 is given implicitly.

Our results are summarized in Tables 2 – 8. In these tables we have used the notation

$\max \Delta$	largest value of $ \Delta y_i^{rel} $ on the relevant interval.
N	Number of nodes used.
Q	Number of nodes where quenching was needed.

P	Number of nodes where local error control in μ_i was primary.
S	Number of nodes where local error control in μ_i was secondary.
★	Number of steps where stepsize control was due to stability considerations (see the later section Stiffness and Stability).
h_2	size of $h_2 = x_2 - x_1$, rounded to first significant digit.
$\max \Delta_E$	largest value of $ \Delta y_i^{rel} $ using the N nodes in RK1 without any error control at all.

Table 2: Numerical results for $\varepsilon_g = 10^{-2}, \varepsilon_\rho = 10^{-4}$

#	max Δ	N	Q	P	S	★	h_2	$\max \Delta_E$
1	9.3×10^{-3}	71	16	0	0	1	1.4×10^{-3}	2.0×10^{-1}
2	8.8×10^{-3}	91	1	0	0	1	1.4×10^{-3}	1.3×10^{-2}
3	9.4×10^{-3}	221	1	0	0	1	1.4×10^{-3}	1.2×10^{-2}
4	6.3×10^{-3}	221	0	0	0	1	1.4×10^{-3}	6.3×10^{-3}
5	8.9×10^{-3}	46	2	0	0	1	1.4×10^{-3}	2.1×10^{-2}
6	9.2×10^{-3}	121	2	0	0	1	1.4×10^{-3}	1.5×10^{-2}

Table 3: Numerical results for $\varepsilon_g = 10^{-4}, \varepsilon_\rho = 10^{-6}$

#	max Δ	N	Q	P	S	★	h_2	$\max \Delta_E$
1	8.0×10^{-5}	88	75	63	0	1	1.4×10^{-3}	1.6×10^{-1}
2	9.2×10^{-5}	91	32	0	0	1	1.4×10^{-3}	1.3×10^{-2}
3	9.4×10^{-5}	221	115	0	0	1	1.4×10^{-3}	1.2×10^{-2}
4	9.5×10^{-5}	223	64	11	0	1	1.4×10^{-3}	5.6×10^{-3}
5	7.9×10^{-5}	63	47	30	8	1	1.4×10^{-3}	1.5×10^{-2}
6	9.4×10^{-5}	121	53	63	0	1	1.4×10^{-3}	1.5×10^{-2}

Table 4: Numerical results for $\varepsilon_g = 10^{-6}, \varepsilon_\rho = 10^{-8}$

#	max Δ	N	Q	P	S	★	h_2	$\max \Delta_E$
1	7.2×10^{-7}	327	324	310	0	1	1.2×10^{-3}	3.9×10^{-2}
2	7.2×10^{-7}	108	91	0	41	1	1.4×10^{-3}	1.0×10^{-2}
3	9.1×10^{-7}	221	211	0	0	1	1.4×10^{-3}	1.2×10^{-2}
4	5.4×10^{-7}	311	308	142	0	1	1.0×10^{-3}	2.1×10^{-3}
5	8.9×10^{-7}	214	209	158	38	1	1.4×10^{-3}	3.9×10^{-3}
6	9.2×10^{-7}	276	251	40	219	1	1.2×10^{-3}	4.0×10^{-3}

Table 5: Numerical results for $\varepsilon_g = 10^{-8}, \varepsilon_\rho = 10^{-10}$

#	max Δ	N	Q	P	S	★	h_2	max Δ_E
1	8.3×10^{-15}	1474	1472	1459	0	1	2.7×10^{-4}	8.6×10^{-3}
2	7.7×10^{-9}	330	323	86	219	0	1.0×10^{-3}	3.4×10^{-3}
3	7.9×10^{-9}	695	692	663	0	0	5.4×10^{-4}	4.8×10^{-3}
4	1.1×10^{-15}	951	949	890	0	0	3.3×10^{-4}	6.5×10^{-4}
5	8.9×10^{-10}	949	946	754	176	1	3.5×10^{-4}	9.0×10^{-4}
6	9.5×10^{-9}	1233	1223	206	1012	1	2.6×10^{-4}	8.9×10^{-4}

Table 6: Numerical results for $\varepsilon_g = 10^{-10}, \varepsilon_\rho = 10^{-12}$

#	max Δ	N	Q	P	S	★	h_2	max Δ_E
1	1.5×10^{-14}	6776	6774	6766	0	0	1.1×10^{-4}	1.9×10^{-3}
2	4.7×10^{-11}	1460	1457	425	1011	0	2.2×10^{-4}	7.6×10^{-4}
3	1.8×10^{-15}	3139	3137	3115	0	0	1.2×10^{-4}	1.1×10^{-3}
4	1.2×10^{-15}	4361	4359	4278	0	0	6.1×10^{-5}	1.5×10^{-4}
5	8.6×10^{-11}	4354	4350	3518	820	0	1.4×10^{-4}	2.0×10^{-4}
6	2.2×10^{-15}	5676	5674	975	4691	0	1.0×10^{-4}	1.9×10^{-4}

Table 7: Numerical results for $\varepsilon_g = 10^{-2}, \varepsilon_\rho = 10^{-3}$

#	max Δ	N	Q	P	S	★	h_2	max Δ_E
1	9.3×10^{-3}	71	16	0	0	1	1.4×10^{-3}	2.0×10^{-1}
2	8.8×10^{-3}	91	1	0	0	1	1.4×10^{-3}	1.3×10^{-2}
3	9.4×10^{-3}	221	1	0	0	1	1.4×10^{-3}	1.2×10^{-2}
4	6.3×10^{-3}	221	0	0	0	1	1.4×10^{-3}	6.3×10^{-3}
5	8.9×10^{-3}	46	2	0	0	1	1.4×10^{-3}	2.1×10^{-2}
6	9.2×10^{-3}	121	2	0	0	1	1.4×10^{-3}	1.5×10^{-2}

Table 8: Numerical results for $\varepsilon_g = 10^{-6}, \varepsilon_\rho = 10^{-7}$

#	max Δ	N	Q	P	S	★	h_2	max Δ_E
1	9.5×10^{-7}	162	159	141	0	1	1.2×10^{-3}	7.9×10^{-2}
2	7.2×10^{-7}	92	75	0	7	1	1.4×10^{-3}	1.2×10^{-2}
3	9.1×10^{-7}	221	211	0	0	1	1.4×10^{-3}	1.2×10^{-2}
4	9.4×10^{-7}	243	240	47	0	1	1.4×10^{-3}	3.6×10^{-3}
5	8.9×10^{-7}	110	106	69	17	1	1.4×10^{-3}	7.9×10^{-3}
6	9.4×10^{-7}	150	137	14	71	1	1.2×10^{-3}	8.3×10^{-3}

In every single case, max Δ is less than ε_g . For any given example, the value of N tends to increase as ε_g is decreased. The number of steps where stepsize

control was due to stability considerations was never more than one for any of the examples. The value of 1.4×10^{-3} for h_2 occurs often; this is explained in the next section. The number of nodes where quenching was needed tends to increase as ε_g is decreased. LEC was not needed at all for $\varepsilon_g = 10^{-2}$, but for all other cases LEC was necessary and, in some cases, at almost every node. Primary LEC occurred more often than secondary LEC, but both types were definitely present. There were, however, some cases where there was no secondary LEC even though primary LEC was needed. We included $\max \Delta_E$ purely for interests' sake - clearly $\max \Delta$ is less than $\max \Delta_E$ for every case, usually by many orders of magnitude (except #4 in Table 2, where no quenching or LEC was required). In Tables 2–6, $\varepsilon_\rho = \varepsilon_g/100$, and in Tables 7 and 8, $\varepsilon_\rho = \varepsilon_g/10$, suggesting that a looser bound on LEC still yields acceptable results (see comments in the Appendix regarding *initial stepsize*).

In Figures 1–10 (for convenience, all figures are collected at the end of the paper, after the Appendix), we show some error curves for two of the examples (#3 and #5) for all five global tolerances considered here. In all of these figures, we adopt the following conventions: horizontal red line is ε_g ; black dots indicate $|\Delta y_i^{rel}|$, the relative global error estimate in the RK1 solution; green curve indicates $|\Delta y_i^T|$, the estimate of the relative global error in y_i^T ; magenta circles indicate the true global error in y_i at those nodes where quenching was not needed; blue circles indicate the true global error in y_i at those nodes where quenching was implemented. Clearly, quenching does not occur when $|\Delta y_i^{rel}|$ dips below ε_g , as expected. In all cases, the true global error in y_i (either magenta circles or blue circles) lies below ε_g , as desired. Note that $|\Delta y_i^T|$ lies above the quenched error, but below ε_g , thus serving the purpose of a good estimator. The exception occurs when $\varepsilon_g = 10^{-10}$, where $|\Delta y_i^T|$ is similar to the quenched error, and both are of the order of machine precision. This probably exposes the limit of the algorithm's capabilities, at least on the computational platform used here [18], perhaps indicating that a tolerance this strict is not practical. We also see that quenching becomes more prevalent as ε_g decreases, because the RK1 solution cannot satisfy such strict tolerances.

Although we only show results for two examples, the other examples exhibit similar behaviour. Of course, details for all the examples are to be found in the tables.

5 Reboot

In Step 9 above, we briefly mentioned the reboot process. In Figure 11, we show the outcome of this process for example #3, for two reboot tolerances, on the interval $[0, 50]$. The reboot tolerance ε_{rb} is the maximum allowed magnitude of $|\Delta y_i^T|$, and the reboot process is designed to prevent $|\Delta y_i^T|$ from becoming too significant with respect to ε_g . In the first of these figures, we use $\varepsilon_{rb} = 10^{-10}$, and in the second we use $\varepsilon_{rb} = 10^{-7}$. It is clear that no reboots were required in the second case, but in the first case nine reboots were needed (the reboots occur whenever $|\Delta y_i^T|$ breaches $\varepsilon_{rb} = 10^{-10}$). Admittedly, the value $\varepsilon_{rb} = 10^{-10}$ is strict, and was chosen for the purpose of demonstration. Ordinarily, we would probably be satisfied with $\varepsilon_{rb} = \varepsilon_g/1000$. For the record, the case $\varepsilon_{rb} = 10^{-7}$ has $N = 521, Q = 125, P = 0, S = 0$ and $\star = 1$, and the case $\varepsilon_{rb} = 10^{-10}$ has $N = 709, Q = 111, P = 27$ and $S = 0$. Each reboot also required a single stepsize adjustment based on stability/stiffness (see next section), giving $\star = 10$.

The reboot process is, effectively, a type of quench. The idea is to restart the integration process at the reboot node x_{rb} with the value of y given by

$$y_{rb} = y_0 + f(\mu_{rb}^V)(x_{rb} - x_0),$$

following which we set new values for the initial point

$$\begin{aligned} x_0 &= x_{rb} \\ y_0 &= y_{rb} \end{aligned}$$

and we proceed from Step 1 described earlier. The reboot node x_{rb} is the node that precedes the node at which $|\Delta y_i^T|$ breaches ε_{rb} . Hence, our reboot process requires a backtrack of only one node. Note that, since we have changed the initial point, we need to determine a new $g(x, \mu)$. We necessarily assume that using μ_{rb}^V in y_{rb} will yield the most accurate value of y_{rb} that we can achieve.

6 Stiffness and Stability

We have

$$\begin{aligned}
g(x, \mu) &= \frac{f(y_0 + f(\mu)(x - x_0)) - f(\mu)}{f_y(\mu)(x - x_0)} \\
&= \frac{f(y_0 + f(\mu)(x - x_0)) - f(y_0 + \mu - y_0)}{f_y(\mu)(x - x_0)} \\
&\approx \frac{f(y_0 + f(\mu)(x - x_0)) - f(y_0) - f_y(y_0)(\mu - y_0)}{\left(\frac{f_y(\mu)}{f(\mu)}\right) f(\mu)(x - x_0)} \\
&= \left(\frac{f(\mu)}{f_y(\mu)}\right) \left(\frac{f(y_0 + f(\mu)(x - x_0)) - f(y_0)}{f(\mu)(x - x_0)}\right) \\
&\quad + \left(\frac{f(\mu)}{f_y(\mu)}\right) \left(\frac{f_y(y_0)(y_0 - \mu)}{f(\mu)(x - x_0)}\right) \\
&\approx \frac{f(\mu) f_y(y_0)}{f_y(\mu)} + \frac{f_y(y_0)(y_0 - \mu)}{f_y(\mu)(x - x_0)} \\
&= \frac{f_y(y_0)}{f_y(\mu)} \left(f(\mu) + \frac{y_0 - \mu}{x - x_0}\right).
\end{aligned}$$

Hence,

$$g_\mu(x, \mu) = -\frac{f_y(y_0) f_{yy}(\mu)}{f_y^2(\mu)} \left(f(\mu) + \frac{y_0 - \mu}{x - x_0}\right) + \frac{f_y(y_0)}{f_y(\mu)} \left(f_y(\mu) - \frac{1}{x - x_0}\right).$$

For $\mu_1 \approx y_0$ we find

$$\begin{aligned}
g_\mu(x_1, \mu_1) &\approx -\frac{f_y(y_0) f_{yy}(y_0)}{f_y^2(y_0)} \left(f(y_0) + \frac{y_0 - y_0}{x_1 - x_0}\right) \\
&\quad + \frac{f_y(y_0)}{f_y(y_0)} \left(f_y(y_0) - \frac{1}{x_1 - x_0}\right) \\
&= -\frac{f_{yy}(y_0) f(y_0)}{f_y(y_0)} + f_y(y_0) - \frac{1}{x_1 - x_0}
\end{aligned}$$

and if $x_1 \approx x_0$ and $y' = f(y)$ is nonstiff or weakly stiff, we would likely find that $\frac{-1}{x_1 - x_0}$ is the dominant term. So,

$$g_\mu(x_1, \mu_1) \approx -\left(\frac{1}{x_1 - x_0}\right) = -1000$$

for the values used in this study. We note that if $f_y(y_0)$ is small and positive, the first term on the RHS could contribute to stiffness in $\mu' = g(x, \mu)$; if

$f_y(y_0)$ is negative the second term contributes to stiffness in $\mu' = g(x, \mu)$; if $f_y(y_0)$ is negative and has suitably small magnitude, the first term could cancel somewhat with the third term, thus reducing the stiffness in $\mu' = g(x, \mu)$.

For the examples considered here, we found

Table 9: μ_1 and $g_\mu(x_1, \mu_1)$

#	y_0	μ_1	$g_\mu(x_1, \mu_1)$
1	2	2.0010	-999.00
2	0.1	0.1000	-999.85
3	1	1.0001	-999.76
4	1	1.0005	-999.99
5	-1	-0.9997	-998.98
6	1	0.8885	-1001.00

consistent with our assumption $\mu_1 \approx y_0$ and our result $g_\mu(x_1, \mu_1) \approx -1000$.

For stability, we demand that, when solving the Dahlquist equation

$$\mu' = -\lambda\mu, \quad \lambda > 0, \quad \mu(0) = \mu_0 = 1$$

using any of the RK methods in DP853, we find a solution at x_1 that has the same properties as the true solution, i.e.

$$0 < e^{-\lambda x_1} < 1.$$

In other words, we demand that if

$$\mu_1 = \mu_0 + h\Phi(x_0, \mu_0),$$

then

$$0 < \mu_1 < 1. \quad (17)$$

Usually, stability with regard to stiffness concerns only the upper bound in this expression, but we have observed that the methods in DP853 yield negative values of μ_1 for some values of h . Hence, we have determined the range of values of h such that both bounds in (17) are satisfied by all three methods in DP853. This has yielded

$$-1.3764 < -\lambda h < 0.$$

For our situation involving $\mu' = g(x, \mu)$, the stiffness constant λ for the step $[x_1, x_2]$ is estimated as

$$\lambda = |g_\mu(x_1, \mu_1)|$$

so that

$$h_2 = \frac{1.3764}{|g_\mu(x_1, \mu_1)|} \approx 1.3764 \times 10^{-3} \quad (18)$$

is the largest value of $h_2 = x_2 - x_1$ that we should be willing to use. This value (rounded to 1.4×10^{-3}) appears numerous times in the tables of results presented earlier, as the value of h_2 that was used. This restriction on the magnitude of the stepsize is performed at every step *prior* to the numerical solution on that step being computed. Any stepsize adjustment via LEC that is subsequently required is, of course, performed *after* the numerical solution on that step has been found.

Note that we do not need to determine the stability regions of DP853 in the complex plane, because we are dealing only with univariate problems in this work. The stability interval $[-1.3764, 0]$ on the negative real axis is all that we require. For systems of differential equations, the stiffness constant would be estimated using the eigenvalues of the Jacobian of the system, which could be complex numbers. In such a case, the entire stability region of each method in DP853 in the complex plane would need to be known.

7 Future Research

We regard this paper as the first in a larger project, and so we have restricted our study to that of scalar, autonomous, nonstiff or weakly stiff problems. We anticipate that future research will address the following:

1. Non-autonomous problems $y' = f(x, y)$, which will require two unknowns, ξ and μ , to be determined for the remainder term. This means that we will need to solve the system

$$\begin{bmatrix} \xi' \\ \mu' \end{bmatrix} = \begin{bmatrix} g_1(x, \xi, \mu) \\ g_2(x, \xi, \mu) \end{bmatrix}.$$

2. Non-autonomous systems

$$\begin{bmatrix} y'_1 \\ \vdots \\ y'_m \end{bmatrix} = \begin{bmatrix} f_1(x, y_1, \dots, y_m) \\ \vdots \\ f_m(x, y_1, \dots, y_m) \end{bmatrix},$$

which we anticipate will yield $m + 1$ equations for each component, giving $m^2 + m$ equations overall that will need to be solved to find the remainder term.

3. The use of *tandem* RK methods instead of DP853. For example, we may use RK2, RK4, and RK7 to generate low-, high- and very high-order solutions for ξ and μ , even if these RK methods are not embedded. If this proves successful, it means that we are not bound to DP853, and that might provide flexibility for the algorithm.
4. Strongly stiff systems must be considered, wherein we might have to utilize the implicit form of RK1 and suitably stable methods in place of DP853. Indeed, we believe our algorithm has a modular character, so that the RK methods we have used could be replaced with other methods that may have properties more suitable to the problem at hand, whilst preserving the structure of the algorithm as a whole. As a matter of record, we have solved the stiff problem $y' = -1000y$ quite easily using our algorithm, although very small stepsizes were needed ($h \sim 10^{-3}$) due to the explicit nature of DP853. Replacing DP853 with A -stable methods might be a useful line of enquiry.
5. The use of low-order RK methods other than Euler's method.
6. Can a stricter estimate of the global error $|\Delta y_i^T|$ be made, and is it necessary to do so?

8 Concluding Comments

We have described a novel algorithm for controlling global error in a stepwise sense. The algorithm exploits the remainder term of a Taylor expansion of the solution, and requires the use of the DP853 triple to solve an auxiliary problem which enables this remainder term to be determined. A quenching process then allows the solution generated by Euler's method to be controlled. We have achieved tolerances on the relative global error as strict as 10^{-10} . Admittedly, we have restricted the calculations in this paper to scalar, autonomous, nonstiff or weakly stiff problems. Naturally, we hope that future research will expand the scope of our algorithm.

References

[1] T. Apostol, *Calculus*, Wiley, 1967.

- [2] R. Aïd, L. Levacher, Numerical investigations on global error estimation for ordinary differential equations, *J. Comput. Appl. Math.*, 82 (1997), 21-39
- [3] E. Boman and R. Rogers, Lagrange's Form of the Remainder, Chapter 5 in *Real Analysis*, LibreTextsTM Mathematics (<https://math.libretexts.org>).
- [4] J.C. Butcher, *Numerical Methods for Ordinary Differential Equations*, Wiley, Chichester, 2003.
- [5] M. Calvo, D.J. Higham, J.I. Montijano, L. Rández, Global error estimation with adaptive explicit Runge–Kutta methods, *IMA J. Numer. Anal.*, 16 (1996), 47-63
- [6] M. Calvo, S. González-Pinto, J.I. Montijano, Global error estimation based on the tolerance proportionality for some adaptive Runge–Kutta codes, *J. Comput. Appl. Math.*, 218 (2008), 329-341
- [7] J.R. Dormand, R.R. Duckers, P.J. Prince, Global error estimation with Runge–Kutta methods, *IMA J. Numer. Anal.*, 4 (1984), 169-184
- [8] J.R. Dormand, M.A. Lockyer, N.E. McGorrigan, P.J. Prince, Global error estimation with Runge–Kutta triples, *Comput. Math. Appl.*, 18 (1989), 835-846
- [9] E. Hairer, S.P. Norsett and G. Wanner, *Solving Ordinary Differential Equations I - Nonstiff Problems*, Springer, Berlin, 2000.
- [10] G.Yu. Kulikov, R. Weiner, Doubly quasi-consistent parallel explicit peer methods with built-in global error estimation, *J. Comput. Appl. Math.*, 233 (2010), 2351-2364
- [11] G.Yu. Kulikov, R. Weiner, Global error estimation and control in linearly-implicit parallel two-step peer W-methods, *J. Comput. Appl. Math.*, 236 (2011), 1226-1239
- [12] G.Yu. Kulikov, Cheap global error estimation in some Runge–Kutta pairs, *IMA J. Numer. Anal.*, 33 (2013), 136-163
- [13] G.Yu. Kulikov, R. Weiner, Variable-stepsize interpolating explicit parallel peer methods with inherent global error control, *SIAM J. Sci. Comput.*, 32 (2010), 1695-1723

- [14] G.Yu. Kulikov, Global error control in adaptive Nordsieck methods, *SIAM J. Sci. Comput.*, 34 (2012), A839-A860
- [15] G.Yu. Kulikov, Adaptive Nordsieck formulas with advanced global error control mechanisms, *Russian J. Numer. Anal. Math. Modelling*, 28 (2013), 321-352
- [16] J. Lang, J.G. Verwer, On global error estimation and control for initial value problems, *SIAM J. Sci. Comput.*, 29 (2007), 1460-1475
- [17] T. Macdougall, J.H. Verner, Global error estimators for order 7, 8 Runge–Kutta pairs, *Numer. Algorithms*, 31 (2002), 215-231
- [18] Intel i7 9700K CPU, Strix Z390-F mainboard, 48GB DDR4 RAM, Windows 10 64-bit, Matlab R2022b.
- [19] J.S.C. Prentice, Enhancing the accuracy of the Taylor polynomial by determining the remainder term, *arXiv.org* (Cornell University Library), 2023, 14p, [arXiv:2302.09216]
- [20] J.S.C. Prentice, General error propagation in the RKGL method, *J. Comput. Appl. Math.*, 228 (2009), 344–354, DOI: 10.1016/j.cam.2008.09.032
- [21] J.S.C. Prentice, Error in Runge–Kutta methods, *International Journal of Mathematical Education in Science and Technology*, 44:3 (2013) 434-442, DOI: 10.1080/0020739X.2012.714492
- [22] J.S.C. Prentice, Stepwise global error control in an explicit Runge-Kutta method using local extrapolation with high-order selective quenching, *Journal of Mathematics Research*, 3, 2 (2011) 126-136
- [23] J.S.C. Prentice, Runge-Kutta Methods: Local error control does not imply global error control, *Journal of Pure and Applied Mathematics: Advances and Applications*, 6, 1 (2011) 71-84; also at [arXiv:1110.5728]
- [24] J.S.C. Prentice, Relative Global Error Control in the RKQ Algorithm for Systems of Ordinary Differential Equations, *Journal of Mathematics Research*, 3, 4 (2011) 59-66
- [25] J.S.C. Prentice, Nyström Methods in the RKQ Algorithm for Initial-value Problems, *arXiv.org* (Cornell University Library), 2011, 7p, [arXiv:1110.6749]

- [26] J.S.C. Prentice, Global Error Control in the Runge-Kutta Solution of a Hamiltonian System, *arXiv.org* (Cornell University Library), 2011, 12p, [arXiv:1111.6996]
- [27] J.S.C. Prentice, Global Error Control in a Lotka-Volterra System using the RKQ Algorithm, *Journal of Mathematical and Computational Science*, 2, 2 (2012) 413-424
- [28] J.S.C. Prentice, Error-induced Stiffness in the Runge-Kutta Solution of a Lotka-Volterra System, *Applied Mathematical Sciences*, 6, 52 (2012) 2599-2604
- [29] J.S.C. Prentice, Event Location and Global Error in Runge-Kutta Methods, *Applied Mathematical Sciences*, 6, 64 (2012) 3163-3167
- [30] J.S.C. Prentice, The Relative Efficiency of Quenching and Reintegration for Global Error Control in Runge-Kutta Methods, *Journal of Mathematical and Computational Science*, 2, 4 (2012) 880-888
- [31] J.S.C. Prentice, False convergence in the nonlinear shooting method, *Journal of Mathematical and Computational Science*, 5, 4 (2015) 454-461
- [32] L.F. Shampine, L.S. Baca, Global error estimates for ODEs based on extrapolation methods, *SIAM J. Sci. Stat. Comput.*, 6 (1985), 1-14
- [33] R.D. Skeel, Thirteen ways to estimate global error, *Numer. Math.*, 48 (1986), 1-20
- [34] M. Spivak, Calculus 3rd ed., Publish or Perish, Houston, 1994.
- [35] R. Weiner, G.Yu. Kulikov, H. Podhaisky, Variable-stepsize doubly quasi-consistent parallel explicit peer methods with global error control, *Appl. Numer. Math.*, 62 (2012), 1591-1603
- [36] R. Weiner, G.Yu. Kulikov, Local and global error estimation and control within explicit two-step peer triples, *J. Comp. Appl. Math.*, 262, (2014), 261-270

9 Appendix

9.1 Newton's Method for μ_1

We must solve

$$y_\mu - y_0 - f(\mu_1)(x_\mu - x_0) = 0$$

for μ_1 . It is not enough to merely solve this equation in the form presented here. Recall from (2) that we actually have

$$y(x_\mu) = y(x_0) + y'(\xi_1, \mu_1)(x_\mu - x_0),$$

where

$$\mu_1 \equiv y(\xi_1).$$

Strictly speaking, then, we must solve

$$F_\xi(\xi_1) \equiv y_\mu - y_0 - y'(\xi_1, y(\xi_1))(x_\mu - x_0) = 0$$

to find ξ_1 . We use Newton's Method in the following manner:

$$\begin{aligned} & \text{Use RK7 on } [x_0, \xi_1^j] \text{ to estimate } y(\xi_1^j) \\ & \text{Use RK7 on } [x_0, \xi_1^j + \delta\xi] \text{ to estimate } y(\xi_1^j + \delta\xi) \\ & F'_\xi(\xi_1^j) = \frac{F_\xi(\xi_1^j + \delta\xi) - F_\xi(\xi_1^j)}{\delta\xi} \\ & \xi_1^{j+1} = \xi_1^j - \frac{F_\xi(\xi_1^j)}{F'_\xi(\xi_1^j)}, \end{aligned}$$

where we use $\xi_1^0 = (x_\mu + x_0)/2$ as the starting value for the Newton iteration. We have used $\delta\xi = 10^{-5}$ in all our calculations, and we found that no more than three Newton iterations were ever needed for all the examples that we have considered. The stopping criterion we used for the iteration scheme was simply

$$|F_\xi(\xi_1^j)| < 10^{-14}.$$

Once we have found an acceptable value for ξ_1 , we use RK7 on $[x_0, \xi_1]$ to estimate $y(\xi_1)$, and we take this estimate to be μ_1 . In the implementations of RK7 here, we used five steps on the relevant intervals. We note that if the problem is strongly stiff, we would probably prefer to use an A -stable RK method instead of RK7.

9.2 Suggested local tolerance and initial stepsize

9.2.1 Local tolerance

Obtain a "quick and dirty" solution for $\mu' = g(x, \mu)$ using an RK method of moderate order, such as RK4 (which has only four internal stages, and so is reasonably efficient for this purpose). Denote this solution (x_j, μ_j) . Assume

that the resulting relative global error in $y_j = y_0 + f(\mu_j)(x_j - x_0)$ is given by

$$\Delta_j^{rel} = \frac{f_y(\mu_j)(x_j - x_0)\delta\mu_j}{\max_j(1, |y_0 + R(x_j, \mu_j)|)} = \frac{f_y(\mu_j)(x_j - x_0)\delta\mu_j}{\max_j(1, |y_0 + f(\mu_j)(x_j - x_0)|)}$$

where $\delta\mu_j$ denotes the global error in μ_j . We demand that this error be equal in magnitude, at most, to the specified global tolerance ε_g . This gives

$$\begin{aligned} \left| \frac{f_y(\mu_j)(x_j - x_0)\delta\mu_j}{\max_j(1, |y_0 + f(\mu_j)(x_j - x_0)|)} \right| &\leq \varepsilon_g \\ \Rightarrow |\delta\mu_j| &\leq \frac{\varepsilon_g \max_j(1, |y_0 + f(\mu_j)(x_j - x_0)|)}{|f_y(\mu_j)(x_j - x_0)|}. \end{aligned}$$

Choose

$$\delta\mu_m \equiv \max_j \left| \frac{\varepsilon_g \max_j(1, |y_0 + f(\mu_j)(x_j - x_0)|)}{|f_y(\mu_j)(x_j - x_0)|} \right|.$$

Assume

$$\delta\mu_m = (x_N - x_0) \varepsilon_\rho$$

and so, using (13),

$$\varepsilon_\rho = \frac{\delta\mu_m}{(x_N - x_0)}$$

is an estimate for the value of ε_ρ consistent with the specified global tolerance ε_g . We also consider a user-defined default value for ε_ρ , denoted ε_ρ^D , and we choose the local tolerance via

$$\varepsilon_\rho = \min \left(\varepsilon_\rho^D, \frac{\delta\mu_m}{(x_N - x_0)} \right).$$

In this study we have generally used $\varepsilon_\rho^D = \varepsilon_g/100$, but we have done some calculations using $\varepsilon_\rho^D = \varepsilon_g/10$ (see Tables 7 and 8).

Lastly, we note that if the problem is strongly stiff, we would probably prefer to use an A -stable RK method instead of RK4.

9.2.2 Initial stepsize

Assuming that DP3 is formally equivalent to a Taylor expansion up to third-order, we treat the fourth-order term

$$\frac{\mu^{(iv)}(x_1, \mu_1) h_2^4}{24}$$

as the numerical error at x_2 obtained using DP3. The relevant stepsize h_2 is estimated from

$$\left| \frac{\mu^{(iv)}(x_1, \mu_1) h_2^4}{24h_2 \max(1, |\mu_1|)} \right| = \left| \frac{\mu^{(iv)}(x_1, \mu_1) h_2^3}{24 \max(1, |\mu_1|)} \right| = \varepsilon_\rho.$$

Using

$$\begin{aligned} \mu^{(iv)} = g''' &= \left(\frac{\partial}{\partial x} + \frac{d\mu}{dx} \frac{\partial}{\partial \mu} \right) \left(\frac{\partial}{\partial x} + \frac{d\mu}{dx} \frac{\partial}{\partial \mu} \right) \left(\frac{\partial}{\partial x} + \frac{d\mu}{dx} \frac{\partial}{\partial \mu} \right) g \\ &= \left(\frac{\partial}{\partial x} + g \frac{\partial}{\partial \mu} \right) \left(\frac{\partial}{\partial x} + g \frac{\partial}{\partial \mu} \right) \left(\frac{\partial}{\partial x} + g \frac{\partial}{\partial \mu} \right) g \end{aligned}$$

gives

$$h_2 = \left| \frac{24 \max(1, |\mu_1|)}{g'''(x_1, \mu_1)} \right|^{\frac{1}{3}}. \quad (19)$$

Naturally, we also specify a default value h_2^D , and we invoke the stability consideration (18), so that

$$h_2 = \min \left(h_2^D, \frac{1.3764}{|g_\mu(x_1, \mu_1)|}, \left| \frac{24 \max(1, |\mu_1|)}{g'''(x_1, \mu_1)} \right|^{\frac{1}{3}} \right).$$

In our calculations we used $h_2^D = 0.1$, and found that the initial stepsize was always set either by (18) or (19).

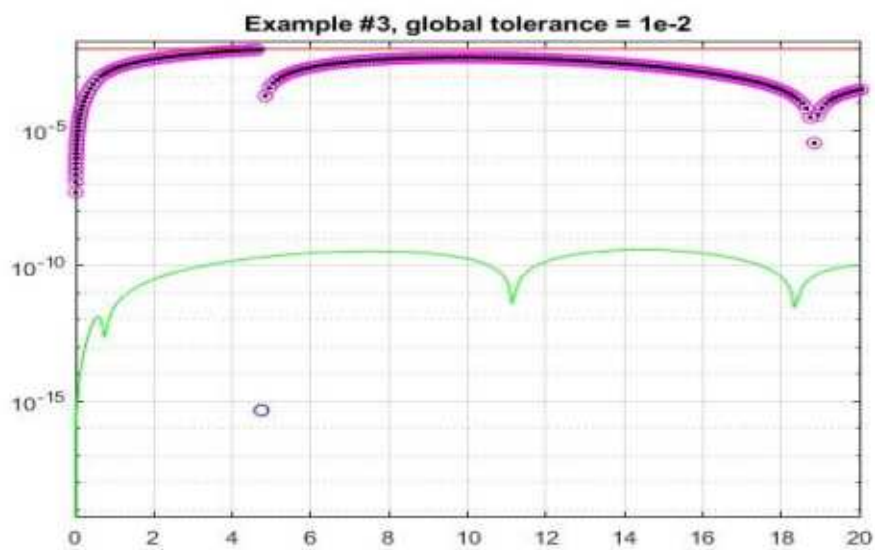


Figure 1

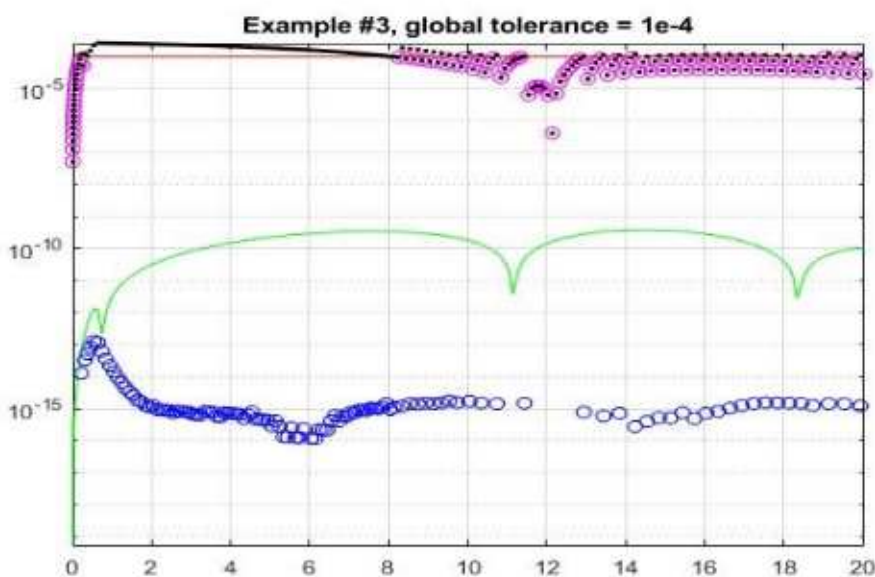


Figure 2

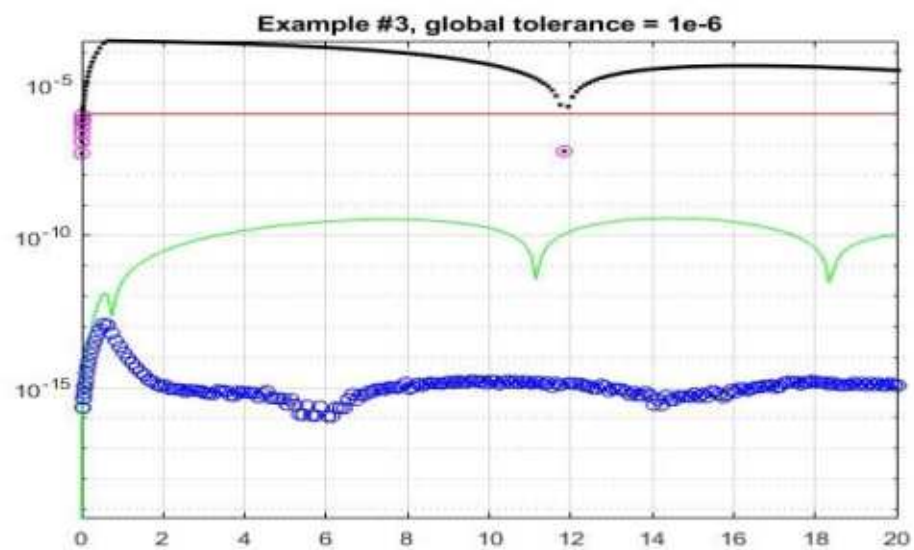


Figure 3

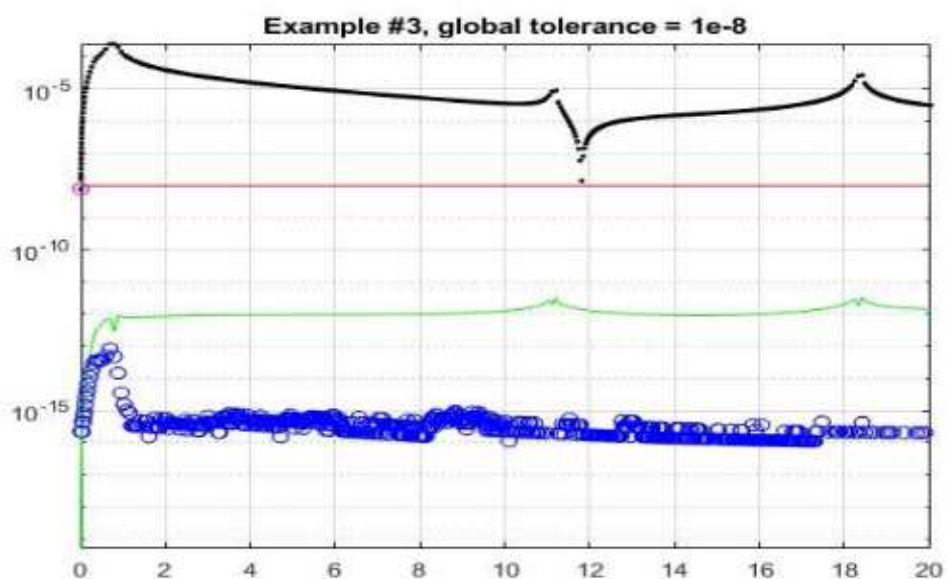


Figure 4

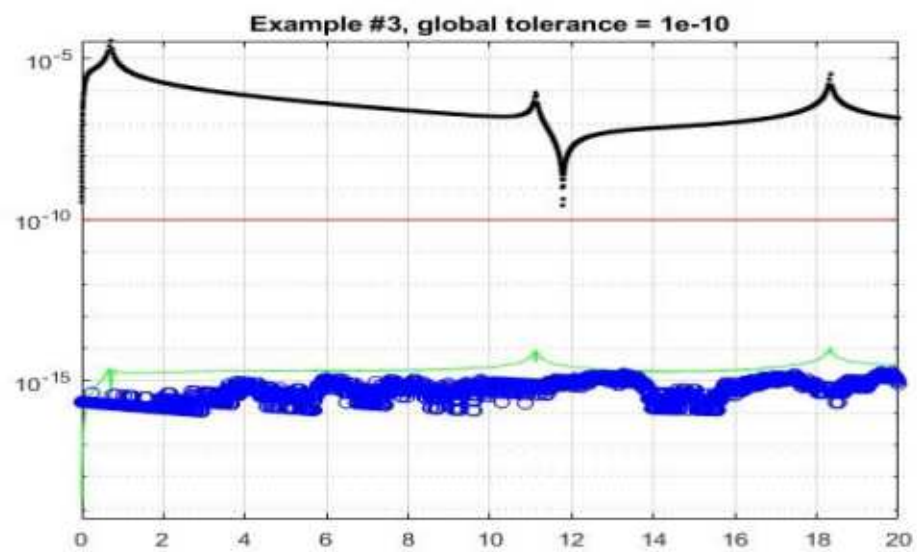


Figure 5

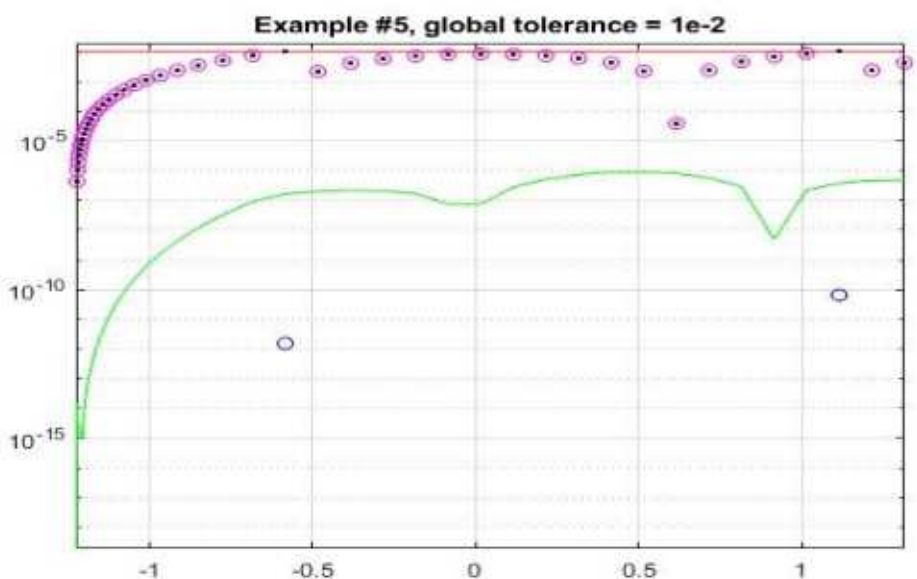


Figure 6

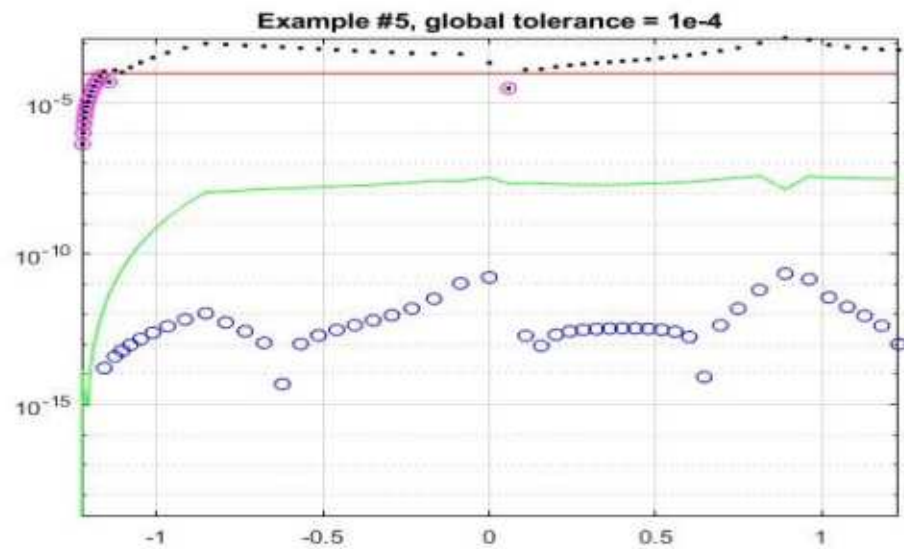


Figure 7

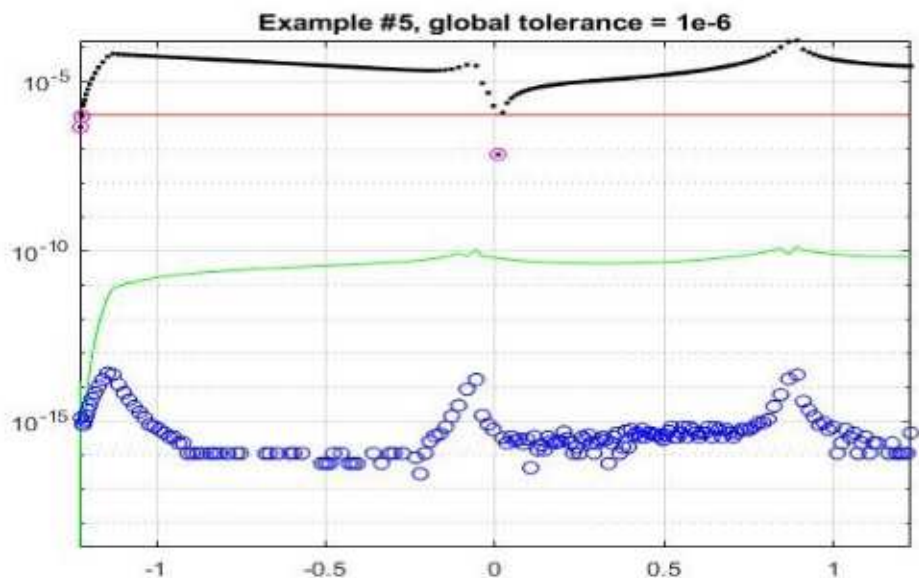


Figure 8

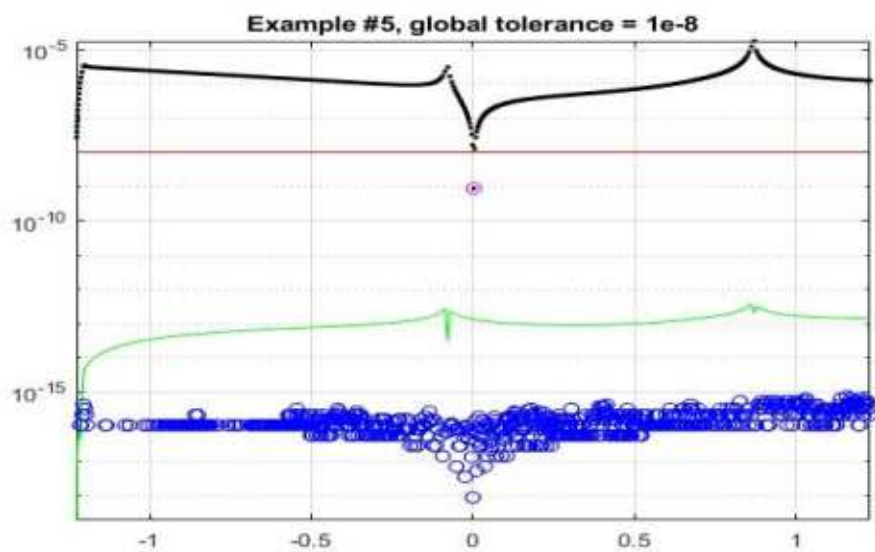


Figure 9

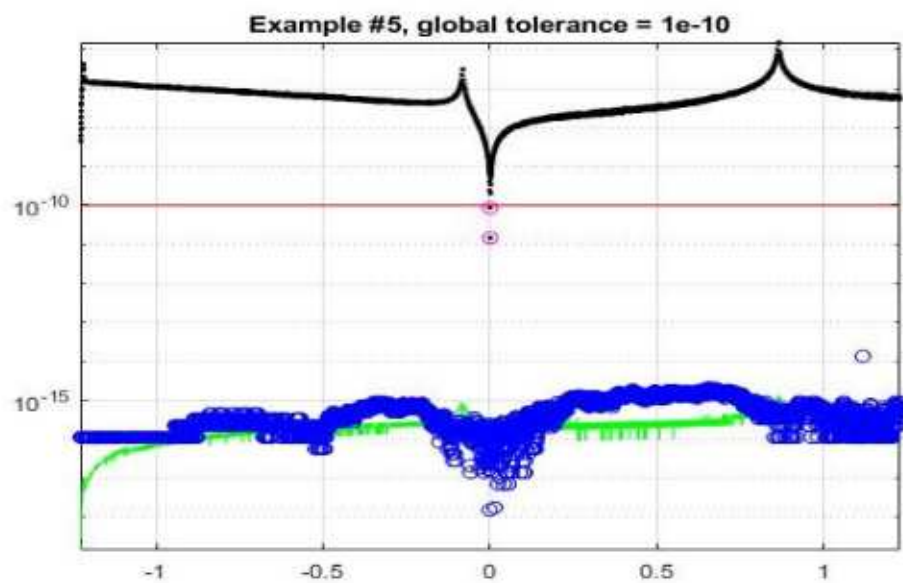


Figure 10

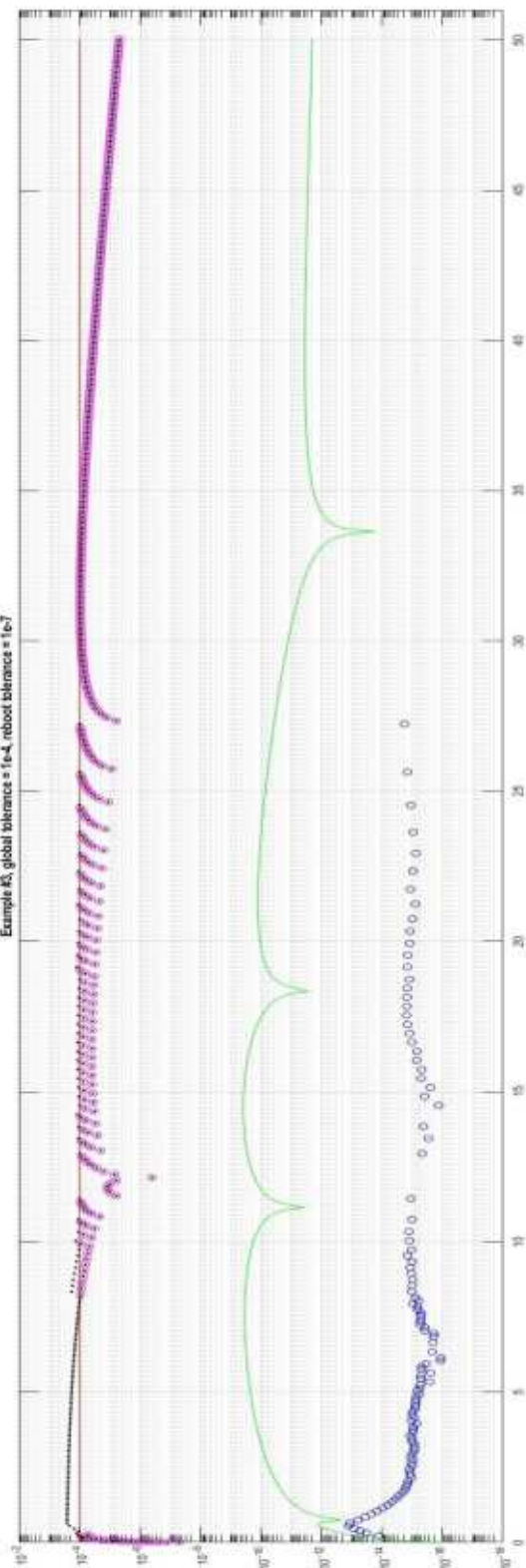
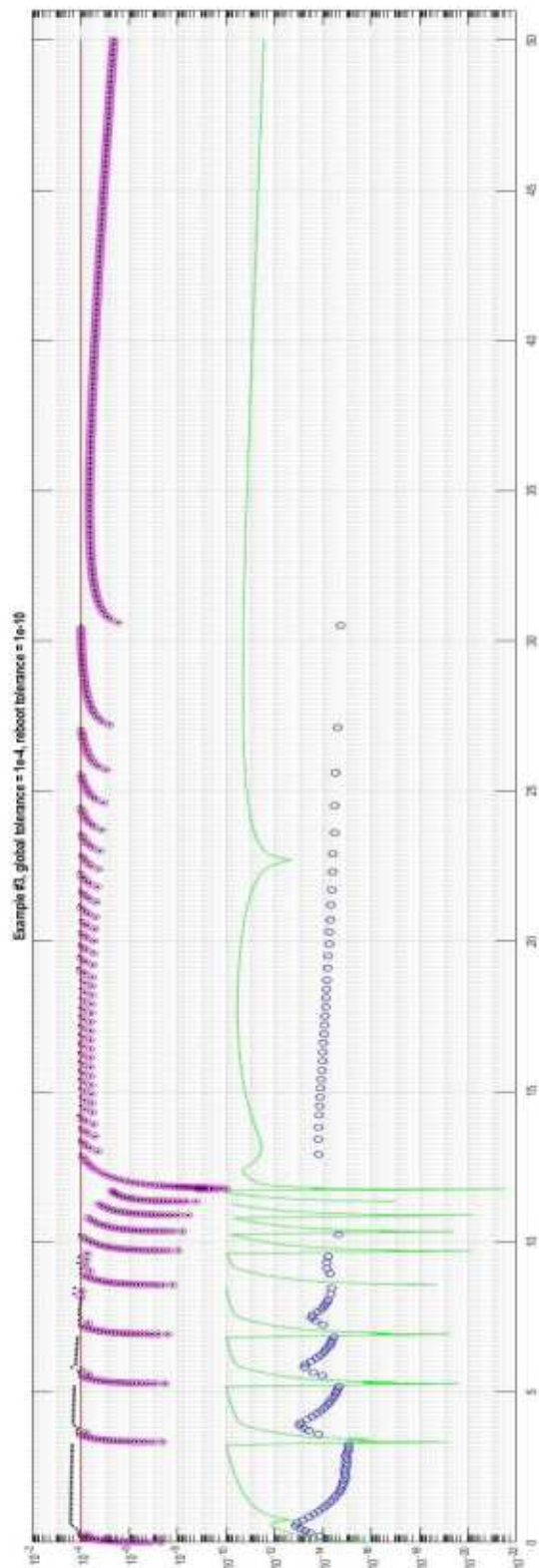


Figure 11